5.2 A MODELING STUDY OF OCEANIC RESPONSE TO DAILY AND MONTHLY SURFACE FORCING

Chung-Hsiung Sui*, Xiaofan Li[1], Michele M. Rienecker, and William K.-M. Lau
NASA/Goddard Space Flight Center, Greenbelt, Maryland
[1]NESDIS, NOAA, Camp Springs, Maryland

1. INTRODUCTION*

The goal of this study is to investigate the effect of high-frequency surface forcing (wind stresses and heat fluxes) on upper-ocean response. We use an updated version of the reduced-gravity quasi-isopycnal ocean model by Schopf and Loughe (1995) including salinity (Yang et al. 1999) for this study. Experiments are performed with daily and monthly surface forcing.

The daily surface wind stress is produced from the SSM/I wind data (Atlas et al. 1991) using a bulk aerodynamic formula. The surface latent and sensible heat fluxes are estimated using the atmospheric boundary layer (ABL) model by Seager et al. (1995) with the time-varying air temperature and specific humidity from the NCEP-NCAR reanalysis. The radiation is based on climatological shortwave radiation from the Earth Radiation Budget Experiment (Harrision et al. 1993) and the daily shortwave radiation budget data produced by Drs. Pinker and Laszlo, University of Maryland (see Pinker and Laszlo 1992 and Laszlo et al. 1997). The ocean model domain is restricted to the Pacific Ocean with realistic land boundaries. At the southern boundary the model temperature and salinity are relaxed to the Levitus (1994) climatology.

2. RESULTS

Four experiments, D1, M1, D2, and M2 are performed. The two experiments, D1 and D2, are subject to daily surface forcing, i.e. wind stress, surface solar radiation, and sensible/latent heat fluxes determined by daily winds and the ABL model. The monthly mean wind stress, solar radiation, and sensible/latent heat fluxes (determined by monthly winds and the ABL model) are used to force the model in experiments M1 and M2. All four experiments are subject to the same monthly mean precipitation (Xie and Arking 1996), and climatological surface longwave radiation. D1 and M1 differ from D2 and M2 primarily in the vertical diffusion parameters.

Generally speaking, the time-mean SST fields and the seasonal to interannual SST variability in the four model experiments agree reasonably well with the observed SST field. The seasonal and interannual heat budgets in the model equatorial mixed layer show that the surface fluxes and horizontal advection dominate the heat budget in the western equatorial Pacific, while surface fluxes and vertical mixing dominate in the eastern Pacific. This is consistent with observations and the model study by Borovikov et al. (1999). The intraseasonal variability of SST and the corresponding heat budget in the equatorial western Pacific from the experiment D1 and D2 compare favorably with the TOGA COARE observations (Cronin and McPhaden 1997).

The model SST variability in the equatorial western Pacific is shown in Fig. 1. The model SSTs forced by monthly surface forcing (M1 and M2) are warmer than those by daily surface forcing (D1 and D2). This is consistent with the results of Rosati and Miyakoda (1988) that is caused by underestimated surface evaporation by the monthly wind speeds in their experiments. Furthermore, the SST variability in M1 and M2 are quite similar to each other, indicating that the model responses to monthly forcing are less sensitive to the change in model vertical mixing parameters. On the other hand, the two experiments forced by daily surface forcing, D1 and D2, differ significantly, indicating a greater sensitivity to the model mixing parameters.

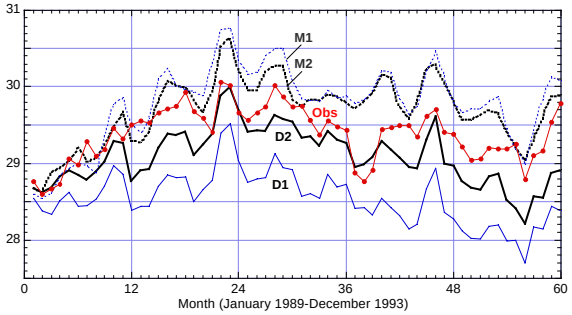

Fig. 1 Time series of SST within (eq, 150°E-170°E).

To identify the processes responsible for the different response between monthly and daily forcing, we examined the heat balance during the

* *Corresponding author address*: C.-H. Sui NASA/GSFC, Mail code 913, Greenbelt, MD 20771; e-mail: sui@climate.gsfc.nasa

first year (when the difference developed) in the experiment D2 and M2. The heat balance in the mixed layer is expresses as

$$h\frac{\partial T}{\partial t} = -h\vec{v}\bullet\nabla T - w_e\frac{\partial T}{\partial \varsigma} + \frac{\partial}{\partial \varsigma}(\frac{\kappa}{h}\frac{\partial T}{\partial \varsigma}) + \frac{\partial Q}{\partial \varsigma} \qquad (1)$$

$$h.adv \; + \; \varsigma.adv \; + \; \varsigma.mixing + \; heat.flux$$

where h is the mixed layer depth, $\vec{v}$ horizontal velocity, ς the generalized vertical coordinate, κ the vertical diffusivity coefficient, Q the heat flux (sensible, latent and radiative fluxes at the surface and penetrative shortwave radiation at the bottom of the mixed layer), w_e entrainment velocity at the base of the mixed layer. The right-hand terms are referred to below as *h.adv*, *ς.adv*, *ς.mixing*, and *heat.flux*, respectively.

The budget differences between D2 and M2 in the equatorial band (2.5°S-2.5°N) are shown in Fig. 2. The results reveal two dominant terms in the difference heat budget. One is the *heat.flux* term. This is mostly due to differences in surface latent heat flux which is larger in D2 than in M2. The other is the difference in vertical diffusive processes in terms *ς.adv* +*ς.mixing*. Horizontal advection is also significant east of 160°W. A larger cooling in D2 than M2 gives rise to a colder SST in D2 that feedback to ABL and causes more evaporative cooling in the following years.

To further evaluate the responsible processes, the base vertical diffusion is increased from D2 to D1. The resultant SST field in D1 becomes significantly cooler than that in D2 due to enhanced vertical entrainment and mixing (figure not shown). The enhanced mixing is apparently caused by high-frequency surface winds because the model SST in M2 and M1 do not show much difference.

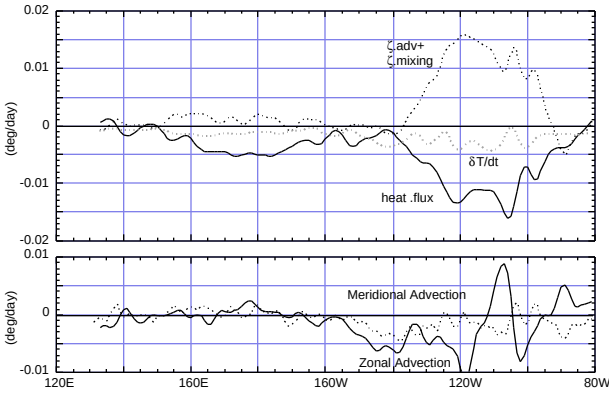

Fig. 2 Difference of first-year (1989) mean heat budget in the mixed layer between D2 and M2 within 2.5°S and 2.5°N.

REFERENCES

Atlas, R., S. C. Bloom, R. N. Hoffman, J. V. Ardizzone, and G. Brin, 1991: Space-based surface wind vectors to aid understanding of air-sea interactions. *Eos, Transactions, Amer. Geoyphys. U*., **72**, 201, 204, 205, and 208.

Borovikov, A., M. M. Rienecker, P. S. Schopf, 1999: Mechanisms for surface warming in the equatorial Pacific ocean during 1994-95. J. Climate (submitted).

Cronin, M. F., and M. J. McPhaden, 1997: The upper ocean heat balance in the western equatorial Pacific warm pool during September-December 1992. *J. Geophys. Res*., **102**, no. C4, 8533-8553.

Harrison, E. F. P. Minnis, B. Barkstrom, and G. Gibson, 1993: Radiation budget at the top of the atmosphere. In Gurney, R. J., Foster, J. L., and Parkinson, C., editors, *Atlas of satellite observations related to global change*, pages 19-38, 1993.

Laszlo, I., R. T. Pinker, and C. H. Whitlock, 1997: Comparison of shortwave fluxes derived from two versions of the ISCCP products, in IRS '96: Current Problems in Atmospheric Radiation, W. Smith (Ed.), A. Deepak Publishing, Hampton, Virginia, USA, 762-765.

Levitus, S., 19982: Climatological Atlas of the World Ocean. NOAA Prof Pap US Government Printing Office, Washington, DC 20402, 73pp.

Pinker, R.T. and I. Laszlo, 1992: Modeling surface solar irradiance for satellite applications on a global scale. *J. Appl. Meteor*., **31**, 194 211.

Rosati, A., and K. Miyakoda, 1988: A general circulation model for upper ocean simulation. *J. Phys. Oceanogr*., **18**, 1601-1626.

Schopf, P. S., and A.Loughe, 1995: A reduced-gravity isopycnal ocean model: Hindcasts of El Nino. *Mon. Wea. Rev*., **123**, 2839-2863.

Seager, R., M. B. Blumenthal, and Y. Kushnir, 1995: An advective atmospheric mixed layer model for ocean modeling purposes: Global simulation of surface heat fluxes. *J. Clim*., **8**, 1951-1964.

Xie, P., P. A. Arkin, 1996: Analysis of global monthly precipitation using gauge observations, satellite estimates and numerical model predictions. *J. Climate*. **9**, 840-858.

Yang, S., K.-M. Lau, and P. S. Schopf, 1999: Sensitivity of the tropical Pacific Ocean to precipitation-induced freshwater flux. *Climate Dynamics*, **15**, 737-750.